Formation and relaxation of excited states in solution: A new time dependent polarizable continuum model based on time dependent density functional theory

Marco Caricato, Benedetta Mennucci, Jacopo Tomasi, Francesca Ingrosso, Roberto Cammi, Stefano Corni, and Giovanni Scalmani

Citation: The Journal of Chemical Physics **124**, 124520 (2006); doi: 10.1063/1.2183309
View online: http://dx.doi.org/10.1063/1.2183309
View Table of Contents: http://scitation.aip.org/content/aip/journal/jcp/124/12?ver=pdfcov
Published by the AIP Publishing

Formation and relaxation of excited states in solution: A new time dependent polarizable continuum model based on time dependent density functional theory

Marco Caricato, Benedetta Mennucci,[a] and Jacopo Tomasi
Dipartimento di Chimica, Università di Pisa, Via Risorgimento 35, 56126 Pisa, Italy

Francesca Ingrosso
Department of Chemistry, Colorado State University, Fort Collins, Colorado 80523-1872

Roberto Cammi
Dipartimento di Chimica, Università di Parma, Viale delle Scienze 17/A, 43100 Parma, Italy

Stefano Corni
INFM-CNR Center on nanoStructures and bioSystems at Surfaces (S3), Via Campi 213/A, 41100 Modena, Italy

Giovanni Scalmani
Gaussian, Inc., Wallingford, Connecticut 06492

(Received 19 December 2005; accepted 10 February 2006; published online 31 March 2006)

In this paper a novel approach to study the formation and relaxation of excited states in solution is presented within the integral equation formalism version of the polarizable continuum model. Such an approach uses the excited state relaxed density matrix to correct the time dependent density functional theory excitation energies and it introduces a state-specific solvent response, which can be further generalized within a time dependent formalism. This generalization is based on the use of a complex dielectric permittivity as a function of the frequency, $\hat{\varepsilon}(\omega)$. The approach is here presented in its theoretical formulation and applied to the various steps involved in the formation and relaxation of electronic excited states in solvated molecules. In particular, vertical excitations (and emissions), as well as time dependent Stokes shift and complete relaxation from vertical excited states back to ground state, can be obtained as different applications of the same theory. Numerical results on two molecular systems are reported to better illustrate the features of the model. © *2006 American Institute of Physics*. [DOI: 10.1063/1.2183309]

I. INTRODUCTION

The accurate modeling of excited state formation and relaxation of molecules in solution is a very important problem in many fields of chemistry and physics. Despite this recognized importance and the numerous applications that such a modeling might have not only in photochemical or spectroscopic studies but also in material science and biology, the progress achieved so far are not as successful as those obtained for ground state phenomena. This delay in the development of accurate but still computationally feasible strategies to study excited states in solution is due to the complexity of the problem in which the processes of formation and relaxation of the electronic state have to be coupled with the dynamics of the solvent molecules.

The study of these phenomena is a research field in which until now the main role has been played by molecular simulation approaches and in particular molecular dynamics. In these last years, however, it has been shown that an alternative and valid strategy is represented by continuum solvation models.[1–3] In these models the solvent is described as a polarizable continuum medium characterized by its dielectric permittivity ε and the solute is represented as a charge distribution inside a cavity within the dielectric.

The formulations of continuum models which have allowed to include a time dependent solvation response can be classified into two main classes. Models belonging to the first class introduce a separation of the solvent polarization into a dynamic contribution, associated with the electronic motion, and an orientational contribution, due to the nuclear and molecular motions.[4–6] Models of the second class implicitly take into account the two contributions in a single response.[7–12]

When the nonequilibrium response following a step change in the solute has to be described, in the methods of the first class the orientational component of the polarization remains in equilibrium with the solute initial state. On the other hand, the dynamic component is assumed to equilibrate instantaneously to the final state. In parallel, methods of the second class represent the solvent response to the step change in the solute, introducing the complex dielectric permittivity as a function of the frequency, $\hat{\varepsilon}(\omega)$. The main difference between the two classes of methods is that the second one can be more easily extended to explicitly include the time dependent evolution of the solvent polarization, i.e., it can be used to model solvation dynamics.

[a]Electronic mail: bene@dcci.unipi.it

The examples of applications of these time dependent versions of continuum models (see references in Ref. 3) until now have been generally limited to some minor aspects of the selected phenomena and not always coupled to efficient quantum-mechanical (QM) computational methods. The reasons for this are strictly linked to a specific aspect of the QM polarizable continuum models. In such models an effective solute Hamiltonian is generally introduced, in which an explicit solvent operator (generally indicated as "reaction field" operator) is added to the solute Hamiltonian. The complexity in this procedure is given by the fact that the solvent reaction field operator is a function of the solute charge distribution and thus nonlinear effects are induced in the effective Hamiltonian. This aspect, which is specific of models in which the solvent polarization explicitly depends on the charge density of the state, introduces an additional complexity when a full inclusion of the coupling between time dependent solvent polarization and the relaxation of the solute electronic state is desired. The consequences of this complexity can be seen in all the steps of the QM description of the excited state formation and relaxation. For example, they can be seen in the calculation of vertical excitation energies, as shown in a recent paper[13] in which we have performed a formal comparison between two of the most widely used QM strategies, namely, the state-specific (SS) method and the linear response (LR) method. We recall that the former solves the effective nonlinear Schrödinger equation for the states of interest (the ground and the excited states) and assumes that the excitation energies can be computed as differences between the corresponding values of the total solute-solvent free energy. By contrast, the latter determines the excitation energies as poles of the frequency dependent linear response functions of the molecular system in the ground state, avoiding explicit calculation of the excited state wave function. The main conclusion of the mentioned paper, from the formal point of view, was that, even in the limit of exact states, the SS and the LR methods applied to polarizable continuum models give different expressions for the excitation energy. In such a comparative paper and in a following one,[14] the origin of the LR-SS difference was imputed to the incapability of the nonlinear effective solute Hamiltonian used in these solvation models to correctly describe energy expectation values of mixed solute states, i.e., states that are not stationary. Since in a perturbation approach such as the LR treatment the perturbed state can be seen as a linear combination of zeroth-order states, the inability of the effective Hamiltonian approach to treat mixed states causes a wrong redistribution of the solvent terms among the various perturbation orders.

In this paper we present a simple but effective strategy (which we shall indicate as "corrected" LR, or cLR) aimed at overcoming this intrinsic limit of the nonlinear effective solute Hamiltonian when applied to LR approaches. With such a strategy a state-specific solvent response is recovered by using a linear response approach. As a result, the LR-SS differences in vertical excitation energies are largely reduced (still keeping the computational feasibility of LR schemes), and the formation and the relaxation of an electronically excited solute can be described in the presence of a time dependent solvent reaction field.

This strategy is based on the use of the integral equation formalism[15] (IEF) version of the polarizable continuum model[16] (PCM) to describe the solvent effects and of a first-order perturbative approach to approximate the nonlinear character of the problem within the time dependent density functional theory (TDDFT). The method used to represent the time dependent evolution of the solvent polarization that follows the transition between two different electronic states in the solute has been obtained as a generalization of the model originally proposed to describe the ground state charge-transfer phenomena within the PCM framework.[17,18] In such a generalization, the recent implementation of analytical derivatives of TDDFT excitation energies is used to calculate the change in the one-particle density matrix of the solute due to an electronic transition and the corresponding change in the solvent reaction field.[19]

The paper is organized as follows. In Sec. II a description of the corrected LR model is presented for the calculation of vertical excitation energies. In Sec. III the approach is extended to the evolution of an excited state from its formation (vertical excitation) to the following emission back to the ground state, and the final relaxation of such a vertical ground state until the initial solute-solvent equilibrium is recovered. For each theoretical section, numerical examples are presented and discussed in Sec. IV. Concluding considerations are reported in Sec. V.

II. A LINEAR RESPONSE APPROACH TO A STATE-SPECIFIC SOLVENT RESPONSE

A. The IEFPCM equations

In the PCM method[15,16] the solvent is represented by a homogeneous continuum medium, which is polarized by the solute placed in a cavity built in the bulk of the dielectric. The solute-solvent electrostatic interactions are described in terms of a solvent reaction potential $\hat{V}_\sigma$, through which we define the main energetic functional to be minimized as

$$\mathcal{G} = \langle\Psi|\hat{H}^0 + \hat{V}_\sigma|\Psi\rangle - \tfrac{1}{2}\langle\Psi|\hat{V}_\sigma|\Psi\rangle. \tag{1}$$

Minimization of $\mathcal{G}[|\Psi\rangle]$ gives the following equation:

$$\hat{H}_{\text{eff}}|\Psi\rangle = [\hat{H}^0 + \hat{V}_\sigma]|\Psi\rangle = E^{\text{GS}}|\Psi\rangle. \tag{2}$$

Within a self-consistent-field (SCF) framework, the solution of this problem leads to the molecular Fock or Kohn-Sham (KS) operator which here becomes

$$F = F^0 + \hat{V}_\sigma, \tag{3}$$

where F^0 collects the gas-phase operators including the one-electron Hamiltonian, Coulomb and (scaled) exchange terms, and possibly the exchange-correlation potential. The remaining solvent induced term $\hat{V}_\sigma$ is expressed as the electrostatic interaction between an apparent charge density σ on the cavity surface, which describes the solvent polarization in the presence of the solute nuclei and electrons. In the computational practice a boundary-element method (BEM) is applied

by partitioning the cavity surface into *Nts* discrete elements, called *tesserae*, and by substituting the apparent surface charge density σ by a collection of point charges q_k, placed at the center of each *tessera* s_k. We thus obtain

$$\hat{V}_\sigma \rightarrow \sum_k^{Nts} \hat{V}_k q(s_k) \quad \text{with } q(s_k) = \sum_l^{Nts} Q_{kl} V(s_l), \tag{4}$$

where $\hat{V}_k$ indicates the electrostatic potential operator computed on the surface element s_k and $V(s_k)$ the corresponding expectation value (including the nuclei contribution). The detailed expression of the **Q** matrix in Eq. (4) depends on the specific version of the PCM method being used and has been previously published (see Ref. 3 for a complete survey) together with efficient ways to solve the associated linear system.[20] Here it is important to recall that **Q** is determined by the form and shape of the cavity, by the partition of the surface, and by the solvent permittivity ε.

The partition of the cavity surface allows us to write Eq. (1) as

$$\mathcal{G}_{GS} = E^{GS} - \tfrac{1}{2}\sum_i V_{GS}(s_i) q_{GS}(s_i), \tag{5}$$

where we have introduced the subscript GS to indicate that the corresponding free energy and solvent charges refer to the solute ground state.

B. Excited state free energy

The free energy expression given in Eq. (1) for a ground state can be generalized to both an equilibrium and a nonequilibrium excited state *K*. In the first case we assume that the solvent reaction field has had time to completely relax from the initial ground state value [determining $\hat{V}_\sigma(\mathrm{GS})$] to the final value representing a new solute-solvent equilibrium [and determining $\hat{V}_\sigma(K)$]. By contrast, in the nonequilibrium regime, the solvent reaction field is represented by a Franck-Condon-type term, sum of an electronic (or dynamic) contribution $\hat{V}_\sigma^{\mathrm{dyn}}(K)$ (in equilibrium with the excited state *K*) and an orientational (or inertial) part still frozen in the initial ground state value, $\hat{V}_\sigma^{\mathrm{in}}(\mathrm{GS})$. The expressions of the free energies corresponding to each regime are described here below.

1. Equilibrium

By defining

$$E_{GS}^K = \langle \Psi_K^{eq} | \hat{H}^0 + \hat{V}_\sigma(\mathrm{GS}) | \Psi_K^{eq} \rangle = \langle \Psi_K^{eq} | \hat{H}^0 | \Psi_K^{eq} \rangle + \sum_i V_K(s_i) q_{GS}(s_i) \tag{6}$$

as the excited state energy in the presence of the fixed reaction field of the ground state $[\hat{V}_\sigma(\mathrm{GS})]$, the free energy becomes

$$\begin{aligned}\mathcal{G}_K^{eq} &= \left\langle \Psi_K^{eq} \middle| \hat{H}^0 + \tfrac{1}{2}\hat{V}_\sigma(K) \middle| \Psi_K^{eq} \right\rangle = E_{GS}^K - \sum_i V_K(s_i) q_{GS}(s_i) \\ &+ \tfrac{1}{2}\sum_i V_K(s_i) q_K(s_i) = E_{GS}^K - \tfrac{1}{2}\sum_i [V_{GS}(s_i) \\ &+ V_i(s_i;\mathbf{P}_\Delta)] q_{GS}(s_i) + \tfrac{1}{2}\sum_i V_{GS}(s_i) q_\Delta(s_i) \\ &+ \tfrac{1}{2}\sum_i V(s;\mathbf{P}_\Delta) q_\Delta(s;\mathbf{P}_\Delta),\end{aligned} \tag{7}$$

where we have expressed the solute electronic density in terms of the one-particle density matrix on a given basis set and rewritten it as a sum of the GS and a relaxation term $\mathbf{P}_\Delta$. This partition automatically implies a parallel partition in the electronic part of the electrostatic potential and in the resulting apparent charges, namely,

$$V_K(s_i) = V_{GS}(s_i) + V(s_i;\mathbf{P}_\Delta),$$

$$q_K(s_i) = q_{GS}(s_i) + q_\Delta(s_i;\mathbf{P}_\Delta).$$

A simplification in the notation can be obtained by exploiting the following approximation:[21]

$$V_{GS}(s_i) q_\Delta(s_i;\mathbf{P}_\Delta) = V(s_i;\mathbf{P}_\Delta) q_{GS}(s_i), \tag{8}$$

which allows to reduce the expression (7) into the following:

$$\mathcal{G}_K^{eq} = E_{GS}^K - \tfrac{1}{2}\sum_i V_{GS}(s_i) q_{GS}(s_i) + \tfrac{1}{2}\sum_i V(s_i;\mathbf{P}_\Delta) q_\Delta(s_i;\mathbf{P}_\Delta). \tag{9}$$

2. Nonequilibrium

The excited state energy in the presence of the fixed reaction field defined in Eq. (6) is now rewritten as

$$E_{GS}^{K,neq} = \langle \Psi_K^{neq} | \hat{H}^0 + \hat{V}_\sigma(\mathrm{GS}) | \Psi_K^{neq} \rangle = \langle \Psi_K^{neq} | \hat{H}^0 | \Psi_K^{neq} \rangle + \sum_i V_K^{neq}(s_i) [q_{GS}^{in}(s_i) + q_{GS}^{dyn}(s_i)], \tag{10}$$

while the free energy becomes

$$\begin{aligned}\mathcal{G}_K^{neq} &= \left\langle \Psi_K^{neq} \middle| \hat{H}^0 + \hat{V}_\sigma^{in}(\mathrm{GS}) + \tfrac{1}{2}\hat{V}_\sigma^{dyn}(K) \middle| \Psi_K^{neq} \right\rangle - \left\langle \Psi_{GS} \middle| \tfrac{1}{2}\hat{V}_\sigma^{in}(\mathrm{GS}) \middle| \Psi_{GS} \right\rangle \\ &= E_{GS}^{K,neq} - \sum_i V_K^{neq}(s_i) q_{GS}^{dyn}(s_i) + \tfrac{1}{2}\sum_i V_K^{neq}(s_i) q_K^{dyn}(s_i) - \sum_i \tfrac{1}{2} V_{GS}(s_i) q_{GS}^{in}(s_i) \\ &= E_{GS}^{K,neq} + \tfrac{1}{2}\sum_i \begin{bmatrix} V_{GS}(s_i) q_{GS}^{dyn}(s_i) + V(s_i;\mathbf{P}_\Delta^{neq}) q_{GS}^{dyn}(s_i) \\ + V_{GS}(s_i) q_\Delta^{dyn}(s_i;\mathbf{P}_\Delta^{neq}) + V(s_i;\mathbf{P}_\Delta^{neq}) q_\Delta^{dyn}(s_i;\mathbf{P}_\Delta^{neq}) \end{bmatrix} \\ &- \sum_i \left[V_{GS}(s_i) q_{GS}^{dyn}(s_i) + V(s_i;\mathbf{P}_\Delta^{neq}) q_{GS}^{dyn}(s_i) + \tfrac{1}{2} V_{GS}(s_i) q_{GS}^{in}(s_i) \right],\end{aligned} \tag{11}$$

where the dynamic and the inertial charges are

$$\mathbf{q}_K^{\mathrm{dyn}} = \mathbf{Q}(\boldsymbol{\epsilon}_\infty)\mathbf{V}_K^{\mathrm{neq}} = \mathbf{Q}(\boldsymbol{\epsilon}_\infty)\mathbf{V}_{\mathrm{GS}} + \mathbf{Q}(\boldsymbol{\epsilon}_\infty)\mathbf{V}(\mathbf{P}_\Delta^{\mathrm{neq}}) = \mathbf{q}_{\mathrm{GS}}^{\mathrm{dyn}} + \mathbf{q}_\Delta^{\mathrm{dyn}},$$

$$\mathbf{q}_K^{\mathrm{in}} = \mathbf{q}_{\mathrm{GS}}^{\mathrm{in}}. \tag{12}$$

By noting that $\mathbf{q}_{\mathrm{GS}}^{\mathrm{in}} + \mathbf{q}_{\mathrm{GS}}^{\mathrm{dyn}} = \mathbf{q}_{\mathrm{GS}}$ we obtain the following:

$$\mathcal{G}_K^{\mathrm{neq}} = E_{\mathrm{GS}}^{K,\mathrm{neq}} + \tfrac{1}{2}\sum_i V(s_i;\mathbf{P}_\Delta^{\mathrm{neq}})q_\Delta^{\mathrm{dyn}}(s_i;\mathbf{P}_\Delta^{\mathrm{neq}}) + \tfrac{1}{2}\sum_i [V_{\mathrm{GS}}(s_i)q_\Delta^{\mathrm{dyn}}(s_i;\mathbf{P}_\Delta^{\mathrm{neq}}) - V(s_i;\mathbf{P}_\Delta^{\mathrm{neq}})q_{\mathrm{GS}}^{\mathrm{dyn}}(s_i)] - \tfrac{1}{2}\sum_i V_{\mathrm{GS}}(s_i)q_{\mathrm{GS}}(s_i). \tag{13}$$

Once again the notation can be simplified if we assume that

$$V_{\mathrm{GS}}(s_i)q_\Delta^{\mathrm{dyn}}(s_i;\mathbf{P}_\Delta^{\mathrm{neq}}) = V(s_i;\mathbf{P}_\Delta^{\mathrm{neq}})q_{\mathrm{GS}}^{\mathrm{dyn}}(s_i),$$

we in fact obtain

$$\mathcal{G}_K^{\mathrm{neq}} = E_{\mathrm{GS}}^{K,\mathrm{neq}} - \tfrac{1}{2}\sum_i V_{\mathrm{GS}}(s_i)q_{\mathrm{GS}}(s_i) + \tfrac{1}{2}\sum_i V(s_i;\mathbf{P}_\Delta^{\mathrm{neq}})q_\Delta^{\mathrm{dyn}}(s_i;\mathbf{P}_\Delta^{\mathrm{neq}}), \tag{14}$$

which is parallel to what has been obtained for the equilibrium case but this time the last term is calculated using the dynamic charges q_Δ^{dyn}.

The vertical transition (free) energy to the excited state K is finally obtained by subtracting the ground state free energy $\mathcal{G}_{\mathrm{GS}}$ of Eq. (5) from $\mathcal{G}_K^{\mathrm{neq}}$ of Eq. (14):

$$\omega_K^{\mathrm{neq}} = \mathcal{G}_K^{\mathrm{neq}} - \mathcal{G}_{\mathrm{GS}} = \Delta E_{\mathrm{GS}}^{K0,\mathrm{neq}} + \tfrac{1}{2}\sum_i V(s_i;\mathbf{P}_\Delta^{\mathrm{neq}})q_\Delta^{\mathrm{dyn}}(s_i;\mathbf{P}_\Delta^{\mathrm{neq}}). \tag{15}$$

C. The corrected linear response approximation

In Eq. (9) [or equivalently in Eq. (14) for the nonequilibrium case] we have shown that excited state free energies can be obtained by calculating the frozen PCM energy E_{GS}^K and the relaxation term of the density matrix, $\mathbf{P}_\Delta$ (or $\mathbf{P}_\Delta^{\mathrm{neq}}$). As said in the Introduction, the calculation of the relaxed density matrices requires the solution of a nonlinear problem being the solvent reaction field dependent on such densities.

If we introduce a perturbative scheme and we limit ourselves to the first order, an approximate but effective way to obtain such quantities is represented by the TDDFT as shown in the following equations.

Using a TDDFT scheme, in fact, we can obtain an estimate of $\Delta E_{\mathrm{GS}}^{K0} = E_{\mathrm{GS}}^K - E^{\mathrm{GS}}$, which represents the difference in the excited and ground state energies in the presence of a frozen ground state solvent as the eigenvalue of the following non-Hermitian eigensystem:

$$\begin{bmatrix} \mathbf{A} & \mathbf{B} \\ \mathbf{B} & \mathbf{A} \end{bmatrix}\begin{bmatrix} X_K \\ Y_K \end{bmatrix} = \omega_K^0 \begin{bmatrix} \mathbf{1} & \mathbf{0} \\ \mathbf{0} & -\mathbf{1} \end{bmatrix}\begin{bmatrix} X_K \\ Y_K \end{bmatrix}, \tag{16}$$

where the orbitals and the corresponding orbital energies used to build $\mathbf{A}$ and $\mathbf{B}$ matrices have been obtained by solving the SCF problem for the effective Fock or KS operator (3), i.e., in the presence of a ground state solvent. The resulting eigenvalue ω_K^0 is a good approximation of $\Delta E_{\mathrm{GS}}^{K0}$ in the sense that it correctly represents an excitation energy obtained in the presence of a PCM reaction field kept frozen in its GS situation, but still it cannot account for the wave function polarization. The consequence is that we cannot distinguish between equilibrium and nonequilibrium wave functions and thus in this approximation $\Delta E_{\mathrm{GS}}^{K0\mathrm{neq}} = \Delta E_{\mathrm{GS}}^{K0} = \omega_K^0$. By using this approximation, the equilibrium and nonequilibrium free energies for the excited state K become

$$\mathcal{G}_K^{\mathrm{eq}} = \mathcal{G}_{\mathrm{GS}} + \omega_K^0 + \tfrac{1}{2}\sum_i V(s_i;\mathbf{P}_\Delta)q_\Delta(s_i;\mathbf{P}_\Delta), \tag{17}$$

$$\mathcal{G}_K^{\mathrm{neq}} = \mathcal{G}_{\mathrm{GS}} + \omega_K^0 + \tfrac{1}{2}\sum_i V(s_i;\mathbf{P}_\Delta^{\mathrm{neq}})q_\Delta^{\mathrm{dyn}}(s_i;\mathbf{P}_\Delta^{\mathrm{neq}}). \tag{18}$$

The only unknown term of Eqs. (17) and (18) is the relaxation part of the density matrix, $\mathbf{P}_\Delta$ (or $\mathbf{P}_\Delta^{\mathrm{neq}}$) (and the corresponding apparent charges q_Δ or q_Δ^{dyn}). These quantities can be obtained through the extension of the TDDFT approach to analytical energy gradients.[22,23] Very recently[19] this extension has been presented also within the PCM scheme. In this extension the so-called Z-vector [24] (or relaxed-density) approach is used. The solution of the Z-vector equation as well as the knowledge of eigenvectors $|X_K, Y_K\rangle$ of the TDDFT linear system allow one to calculate $\mathbf{P}_\Delta$ for each state K as

$$\mathbf{P}_\Delta = \mathbf{T}_K + \mathbf{Z}_K, \tag{19}$$

where $\mathbf{T}_K$ is the unrelaxed density matrix with elements given in terms of the vectors $|X_K, Y_K\rangle$, whereas the Z-vector contribution $\mathbf{Z}_K$ accounts for orbital relaxation effects.

Once $\mathbf{P}_\Delta$ is known we can straightforwardly calculate the corresponding apparent charges as

$$\mathbf{q}_\Delta^x = \mathbf{Q}(\boldsymbol{\epsilon}_x)\mathbf{V}(\mathbf{P}_\Delta^x), \tag{20}$$

where

$$\begin{cases} \epsilon_x = \epsilon \\ \mathbf{P}_\Delta^x = \mathbf{P}_\Delta \\ \mathbf{q}_\Delta^x = \mathbf{q}_\Delta \end{cases} \quad \text{if an equilibrium regime is assumed}$$

$$\begin{cases} \epsilon_x = \epsilon_\infty \\ \mathbf{P}_\Delta^x = \mathbf{P}_\Delta^{\mathrm{neq}} \\ \mathbf{q}_\Delta^x = \mathbf{q}_\Delta^{\mathrm{dyn}}. \end{cases} \quad \text{if a nonequilibrium regime is assumed}$$

By introducing the TDDFT relaxed density (19) and the corresponding charges (20) into Eqs. (17) and (18) we obtain the first-order approximation to the "exact" free energy of the excited state by using a linear response scheme. This is exactly what we have called corrected linear response approach (cLR).

We have efficiently implemented the cLR approach in the development version of the GAUSSIAN program[25] by solving twice the TDDFT equations. First, the explicit solvent contribution is left out from such equations and thus the ω_K^0 excitation energies are computed. Then these solutions are used as a guess to solve the TDDFT equations again, but this time the explicit solvent contribution is included and the corresponding relaxed density is computed and used as detailed

above. This procedure thus allows to compute the cLR excitation energies in a single calculation.

As a final comment, we note that the theory has been here presented for a DFT description, but the same formulation can be equivalently applied to the parallel Hartree-Fock approach either in the complete (random phase approximation) or approximated [Tamm-Dancoff approximation or configuration interaction (CI) singles, CIS] version.

III. TIME DEPENDENT SOLVATION

In this section we extend the corrected LR model described in the previous section to explicitly account for the time dependent (TD) evolution of the solvent polarization. The basic idea beyond this extension is that in a linear response approximation the solvent polarization at a given time due to a TD electric field can be expressed as a convolution integral on previous times as[26]

$$P(t) = \int_{-\infty}^{t} dt' \chi(t-t')E(t'),$$

where $\chi(t)$ is the solvent response function.

If we apply this scheme to the time dependent evolution of the solvent polarization after a vertical excitation from an equilibrated ground state to an excited state K and we reformulate the problem within the PCM framework, the equation to consider is that defining the TD apparent charges, namely,

$$q(t) = \int_{-\infty}^{t} dt' R(t-t')V(t') \Rightarrow \mathbf{q}_K(t) = \mathbf{q}_{GS} + \delta\mathbf{q}_K(t), \quad (21)$$

where we have rewritten the time dependence of the potential as the sum of the ground state potential and a time dependent term: $\mathbf{V}(t)=\mathbf{V}_{GS}+\Delta\mathbf{V}(t)$.

It is convenient to report here the boundary conditions for the charge $\mathbf{q}_K(t)$:

$$\mathbf{q}_K(-\infty) = \mathbf{q}_{GS},$$

$$\mathbf{q}_K(+\infty) = \mathbf{q}_K = \mathbf{q}_{GS} + \mathbf{q}_\Delta, \quad (22)$$

where at $(t\rightarrow-\infty)$ the solvent is in equilibrium with a ground state solute and at $t\rightarrow\infty$ a new equilibrium is reached between solvent and an excited state solute.

A. The TDPCM model

In two recent papers[17,18] we have shown that the general linear response equation (21) can be transformed into a working equation by introducing a simplified expression for the potential time dependence $[\Delta\mathbf{V}(t)]$, namely, as a step function, $\Delta\mathbf{V}(t)=\theta(t)\Delta\mathbf{V}$, where $\Delta\mathbf{V}=\mathbf{V}_K^{eq}-\mathbf{V}_{GS}=\mathbf{V}(\mathbf{P}_\Delta)$. In this approximation, in fact, the variation of the polarization charges $\delta\mathbf{q}_K$ at time t due to a change in the electrostatic potential at time $t=0$ becomes

$$\delta\mathbf{q}_K(\Delta\mathbf{V},t) = \Delta\mathbf{q} + \delta'\mathbf{q}_K(\Delta\mathbf{V},t), \quad (23)$$

$$\delta'\mathbf{q}_K(\Delta\mathbf{V},t) = -\frac{2}{\pi}\int_0^\infty \frac{d\omega}{\omega}\,\mathrm{Im}[\mathbf{R}(\omega)]\cos(\omega t)\Delta\mathbf{V}, \quad (24)$$

where $\Delta_\mathbf{q}=(\mathbf{q}_K-\mathbf{q}_{GS})$ and $\mathbf{R}$ is the PCM response matrix (in the following, for simplicity's sake we shall omit the explicit dependence of $\delta\mathbf{q}_K$ on $\Delta\mathbf{V}$). This expression is obtained passing from the time domain to the frequency domain as required by the form of the dielectric response of the solvent, given in terms of its complex dielectric permittivity $\hat{\varepsilon}$ as a function of the frequency ω. The ω dependence of $\hat{\varepsilon}$ can either be modeled using pure diffusive expressions (as in the Debye relaxation expression) or calculated on the basis of experimental measurements of the absorption in the far-infrared region, combined with the diffusive relaxation at low frequencies. The latter methodology has the advantage of a more correct representation of the short time scale of the solvent response.

If we apply a reversible (in the thermodynamic sense) charging process that leads to the proper solute density in the excited state K and to the proper time dependent solvent charges we can reformulate the expression given in Eq. (11) within the present TDPCM formalism; the resulting time dependent free energy expression becomes

$$\mathcal{G}_K(t) = E_K^0 + \tfrac{1}{2}\sum_i V_K(s_i;\mathbf{P}_K[t])q_K(s_i;t) - \tfrac{1}{2}\sum_i \tilde{V}(s_i;t)\delta' q_K(s_i;t), \quad (25)$$

where we have neglected the time dependence of the polarization of the excited state wave function as in the vacuum term (namely, $\langle\Psi_K[t]|\hat{H}^0|\Psi_K[t]\rangle \simeq \langle\Psi_K[+\infty]|\hat{H}^0|\Psi_K[+\infty]\rangle = E_K^0$ for all t). In Eq. (25) we have also introduced the square parentheses to indicate a parametric dependence on time. In our first-order model, in fact, the variable time is present only in the constitutive equation of the PCM charges (23). These charges are then used as fixed external charges (but changing with time) in the various calculations (one for each time) giving $\mathbf{P}_\Delta[t]$, which has thus only a parametric dependence on time.

In Eq. (25) the last term on the right hand side accounts for the energy spent to polarize the orientational degrees of freedom of the solvent and $\tilde{V}(t)$ is the potential that would generate the orientational part of the PCM charges $[\tilde{V}(t=0) = V_{GS}$ and $\tilde{V}(t=+\infty)=V_K]$. We note that the function $\mathcal{G}_K(t)$ satisfies the following conditions:

$$\mathcal{G}_K(t) \xrightarrow{t\rightarrow 0} \mathcal{G}_K^{neq},$$

$$\mathcal{G}_K(t) \xrightarrow{t\rightarrow +\infty} \mathcal{G}_K^{eq},$$

where $\mathcal{G}_K^{neq}$ is defined in Eq. (14) and $\mathcal{G}_K^{eq}$ is defined in Eq. (9). The first relation can be justified considering that at $t=0$, the charges defined in Eq. (21) become

$$\delta'\mathbf{q}_K(t) \xrightarrow{t\rightarrow 0} \mathbf{q}_{GS}^{in} - \mathbf{q}_K^{in},$$

$$\mathbf{q}_K(t) \xrightarrow{t\to 0} \mathbf{q}_{\mathrm{GS}}^{\mathrm{in}} - \mathbf{q}_K^{\mathrm{dyn}}. \tag{26}$$

From a practical point of view it is useful to rewrite Eq. (25) in an alternative form by introducing a time dependent transition energy $\Delta U_{K0}(t)$, namely,

$$\mathcal{G}_K(t) = \mathcal{G}_{\mathrm{GS}} + \Delta U_{K0}(t), \tag{27}$$

where $\mathcal{G}_{\mathrm{GS}}$ is the equilibrium free energy of the ground state given in Eq. (1) and

$$\Delta U_{K0}(t) = \Delta E_{\mathrm{GS}}^{K0} + \tfrac{1}{2}\sum_i V(s_i;\mathbf{P}_\Delta[t])q_\Delta(s_i;t) + \tfrac{1}{2}\sum_i [V_{\mathrm{GS}}(s_i) - \tilde{V}(s_i;t)]\delta' q(s_i;t), \tag{28}$$

where $\Delta E_{\mathrm{GS}}^{K0} = \omega_K^0$ (see Sec. II C) and $\mathbf{q}_\Delta(t) = \mathbf{q}_\Delta + \delta'\mathbf{q}_K(t)$.

B. Time dependent Stokes shift

One of the applications of the dielectric relaxation model that we propose is the calculation of the solvation response related to an experimentally accessible observable, the time dependent Stokes shift $S(t)$ (TDSS). In experiments, the time evolution of the solvent orientational response is evaluated from the time dependent shift of the solute maximum fluorescence signal $\nu(t)$ with respect to its equilibrium value $\nu(\infty)$:[27]

$$S(t) = \frac{\nu(t) - \nu(\infty)}{\nu(0) - \nu(\infty)}, \tag{29}$$

where $\nu(0)$ is the value corresponding to the vertical transition.

During dielectric relaxation, the fluorescence shift is influenced by the solvent due to the presence of electrostatic, time dependent solute-solvent interactions. The shift of the solute fluorescence therefore contains information about the solvent reorganization process. If the geometry of the solute is subject to negligible changes during the transition, it is possible to express $S(t)$ in terms of the difference between the time dependent solvation energy in the excited state and in the ground state.

According to our description of the phenomenon, the evolution with time of the excited state energy and the PCM charges can be obtained as shown in the previous section and for each time t we model a vertical ground state as

$$\mathcal{G}_{\mathrm{GS}}^{\mathrm{vert}}(t) = E^0 + \tfrac{1}{2}\sum_i V(s_i;\mathbf{P}_{\mathrm{GS}}[t])q_{\mathrm{GS}}^{\mathrm{dyn}}(s_i) - \tfrac{1}{2}\sum_i \tilde{V}(s_i;t)q_K^{\mathrm{in}}(s_i;t) + \sum_i V(s_i;\mathbf{P}_{\mathrm{GS}}[t])q_K^{\mathrm{in}}(s_i;t), \tag{30}$$

where

$$E^0 = \langle\Psi|\hat{H}^0|\Psi\rangle,$$

$$\mathbf{q}_K^{\mathrm{in}}(t) = \mathbf{q}_K(t) - \mathbf{q}_K^{\mathrm{dyn}},$$

$$\mathbf{q}_x^{\mathrm{dyn}} = \mathbf{Q}(\epsilon_\infty)\mathbf{V}(\mathbf{P}_x) \quad \text{with } x = \mathrm{GS}, K. \tag{31}$$

In Eqs. (30) and (31) we have used the same notation used in Eq. (25) to indicate a parametric dependence on time through square parentheses. Here such a parametric dependence applies not only to the excited state but also to the vertical ground state: the energy of such a state in fact is obtained by using fixed (but changing with time) orientational PCM charges $\mathbf{q}_K^{\mathrm{in}}(t)$ in the proper Fock (or KS)operator. It is worth noting that these charges $\mathbf{q}_K^{\mathrm{in}}(t)$ in Eq. (31), which represent the orientational part of the polarization, do not derive from an equilibrium situation, as in usual absorption processes, but at each time t the emission starts from a nonequilibrated excited state.

The time dependent emission frequency is finally obtained by subtracting from $\mathcal{G}_{\mathrm{GS}}^{\mathrm{vert}}(t)$ the corresponding values of $\mathcal{G}_K(t)$, defined in Eq. (27), calculated at the same t.

C. Cyclic relaxation

By applying the TDPCM model, we can follow the complete evolution of an electronic excitation in the solute starting from the vertical transition from an initial solute-solvent equilibrium situation in the ground state, and going back to the ground state, considering the relaxation of both solute geometry and solvent polarization. The overall process can be represented as a six-step cycle as follows:

- Step 1: Electronic excitation of the solute. Solute and solvent are in a nonequilibrium situation, where the solvent is only partially equilibrated with the new charge distribution of the excited solute.
- Step 2: The solvent relaxes towards a new equilibrium, with the solute electronic excited state still maintaining the ground state geometry.
- Step 3: The geometry of the solute relaxes towards its new equilibrium structure together with the solvent.
- Step 4: The solute emits, returning to the electronic ground state. The solvent is again in a (reversed) nonequilibrium situation.
- Step 5: The solvent relaxes towards a new equilibrium, with the solute electronic ground state frozen in the excited state geometry.
- Step 6: The solute geometry relaxes towards the ground state equilibrium structure together with the solvent reaching again the initial equilibrium situation.

In our model, the explicit time evolution of the solvent relaxation is separated (or decoupled) from the relaxation of the solute geometry; the latter thus has to be evaluated in the presence of a completely equilibrated solvent or alternatively in a nonequilibrium solvent. Here, in particular, we shall assume that the geometry relaxation is a process which occurs in a sufficiently long time for the solvent to be always in equilibrium.

The first three steps represent the evolution of the solute excited state. Steps 1 and 2 are described following the time evolution of $\mathcal{G}_K(t)$ in Eq. (27), where the electronic excitation

occurs at $t=0$, whereas step 3 is described by a geometry optimization of the excited state solute in the presence of an equilibrated solvent, which is equivalent to considering the dielectric relaxation to be faster than the solute geometry relaxation. Such an assumption has to be verified for the system of interest, and, in all cases where it is not valid, steps 2 and 3 need to be inverted.

Steps 4–6 describe the evolution of the system when the solute returns to the ground state. For steps 4 and 5 we introduce the ground state analog of the time dependent energy function (25) as [see also the definition of $U^{\mathrm{neq}}(t)$ in the reference paper[18]]:

$$\mathcal{G}_{\mathrm{GS}}(t) = E^0 + \tfrac{1}{2}\sum_i V(s_i;\mathbf{P}_{\mathrm{GS}}[t])q_{\mathrm{GS}}(s_i;t) - \tfrac{1}{2}\sum_i \tilde{V}_{\mathrm{GS}}(s_i)\delta' q_{\mathrm{GS}}(s_i;t), \tag{32}$$

where

$$\mathbf{q}_{\mathrm{GS}}(t) = \mathbf{q}_X + \delta\mathbf{q}_{\mathrm{GS}}(t) = \mathbf{q}_K + [\Delta\mathbf{q}_{\mathrm{GS}} + \delta'\mathbf{q}_{\mathrm{GS}}(t)] = \mathbf{q}_{\mathrm{GS}} + \delta'\mathbf{q}_{\mathrm{GS}}(t) \tag{33}$$

and the charges $\delta\mathbf{q}_{\mathrm{GS}}(t)$ are calculated with the step potential $\Delta\mathbf{V}=-\mathbf{V}(\mathbf{P}_\Delta)$, thus $\delta\mathbf{q}_{\mathrm{GS}}(t)=-\delta\mathbf{q}_K(t)$. In Eq. (32) the last term has the same origin of the analogous term in Eq. (25), but in this case $\tilde{V}_{\mathrm{GS}}(t=0)=V_K$ and $\tilde{V}_{\mathrm{GS}}(t=+\infty)=V_{\mathrm{GS}}$.

The free energy $\mathcal{G}_{\mathrm{GS}}(t)$ in Eq. (32) is different from $\mathcal{G}^{\mathrm{vert}}_{\mathrm{GS}}$, defined in Eq. (30), since the former represents the time dependent evolution of an initial nonequilibrium ground state following the emission from an equilibrated excited state, whereas the latter always represents a vertical ground state following from the instantaneous emission from a time dependent excited state. We also note that at $t=0$, both the charges in Eq. (33) and the energy in Eq. (32) reduce to PCM nonequilibrium charges and free energy, respectively, e.g.,

$$\mathbf{q}_{\mathrm{GS}}(t) \xrightarrow{t\to 0} (\mathbf{q}^{\mathrm{in}}_{\mathrm{GS}} + \mathbf{q}^{\mathrm{in}}_{\Delta}) + \mathbf{q}^{\mathrm{dyn}}_{\mathrm{GS}}$$

and

$$\mathcal{G}_{\mathrm{GS}}(t) \xrightarrow{t\to 0} \mathcal{G}^{\mathrm{neq}}_{\mathrm{GS}} = E^0 + \tfrac{1}{2}\sum_i V(s_i;\mathbf{P}_{\mathrm{GS}}[0])q^{\mathrm{dyn}}_{\mathrm{GS}}(s_i) - \tfrac{1}{2}\sum_i [V^{\mathrm{eq}}_K(s_i)(q^{\mathrm{in}}_\Delta(s_i) + q^{\mathrm{in}}_{\mathrm{GS}}(s_i)) + V(s_i;\mathbf{P}_{\mathrm{GS}}[0])(q^{\mathrm{in}}_\Delta(s_i) + q^{\mathrm{in}}_{\mathrm{GS}}(s_i))],$$

where we have used the following relation:

$$V^{\mathrm{eq}}_K(s_i)q^{\mathrm{in}}_{\mathrm{GS}}(s_i) = V(s_i;\mathbf{P}_{\mathrm{GS}}[0])q^{\mathrm{in}}_{\mathrm{GS}}(s_i) + V(s_i;\mathbf{P}_\Delta)q^{\mathrm{in}}_{\mathrm{GS}}(s_i) = V(s_i;\mathbf{P}_{\mathrm{GS}}[0])q^{\mathrm{in}}_{\mathrm{GS}}(s_i) + V(s_i;\mathbf{P}_{\mathrm{GS}}[0])q^{\mathrm{in}}_\Delta(s_i).$$

Finally, step 6 represents the relaxation of the solute geometry to the initial equilibrium situation (once again the relaxation of the solvent is considered faster than the solute geometry relaxation).

By making use of steps 1–6 we complete the description of electronic excitation and emission of a molecule in solution accounting for the real dynamics of the solvent response.

IV. NUMERICAL EXAMPLES

In this section we present some applications of the corrected linear response and its generalization to time dependent solvation described in Secs. II and III, respectively. For this study we have used the same physical systems [methylen-cyclopropene (MCP) and acrolein (ACRO) in two solvents, an apolar (dioxane) and a polar one (acetonitrile)] studied in the already quoted paper on the differences between LR and SS approaches for effective Hamiltonian methods.[13]

The selected transitions can be seen as representative examples of different types of electronic transitions for which different solvent responses can be studied: the first $\pi\rightarrow\pi^*$ transition for MCP, and the first $n\rightarrow\pi^*$ and $\pi\rightarrow\pi^*$ transitions for ACRO. We note that in MCP the resulting excited state is characterized by a dipole moment which has an opposite direction with respect to that of the ground state, whereas in ACRO, the $n\rightarrow\pi^*$ and $\pi\rightarrow\pi^*$ transitions are characterized by a decrease and an increase in the dipole moment passing from the ground state to the excited state, respectively.

To compare with the results reported in the reference paper, calculations have been performed using the same basis set, namely, the Dunning double ζ basis set with additional $d(0.2)$ function for C, N, and O (the number in parentheses is the exponent of the extra function) and the same molecular cavity for all the systems. The sphere radii used to build the molecular cavity were 1.9 for CH, 2.0 for CH_n $(n=2,3)$, 1.7 for other C, 1.52 for O, 1.6 for N, and 1.2 for H when bonded to N, all multiplied by a cavity size factor of 1.2.

For the first part of the study, focused on vertical (nonequilibrium) absorptions, both TDDFT and CIS calculations have been used, whereas in the successive applications to TDSS and cyclic relaxation processes, the results refer to TDDFT only; in all cases the B3LYP hybrid functional has been used.

Ground state geometries have been taken from the reference paper, while TDDFT analytical gradients (at the B3LYP level with the modified Dunning basis set) have been used to obtain excited state geometries.

All the calculations have been carried out using a development version of GAUSSIAN.[25]

A. Vertical excitations

In this section we compare the results obtained for the vertical (nonequilibrium) absorption process with the standard linear response and its corrected version with respect to those obtained with the reference state-specific approach.

As it is not possible to obtain TDDFT-SS results, the simplest, yet meaningful, possibility is to revert to the CIS method. In fact, this method can be obtained from two points of view: one is to consider the method as a standard CI, in which the wave function of the excited state is constructed

TABLE I. Absorption energies (eV) at HF/CIS level obtained using linear response (LR), state specific (SS), and correlated linear response (cLR) approaches. SS data are taken from Ref. 13.

	MCP ($\pi\pi^*$)		ACRO ($n\pi^*$)		ACRO ($\pi\pi^*$)	
ΔE^{gas}	5.65		4.30		6.91	
	Dioxane	ACN	Dioxane	ACN	Dioxane	ACN
$\Delta E_{\text{GS}}^{K0,\text{neq}}$	5.75	5.89	4.47	4.63	6.91	6.83
LR	5.70	5.85	4.46	4.63	6.63	6.61
cLR	5.62	5.79	4.40	4.58	6.90	6.81
SS	5.51	5.70	4.37	4.57	6.88	6.80

by single excitations from the HF determinant and thus a SS solvent response can be obtained; the other is to consider CIS as the result of the Tamm-Dancoff approximation applied to the linear response equation based on the HF wave function. The two ways of looking at the CIS method give the same equations *in vacuo*, but, as we have discussed in the Introduction, they differ for molecules in solution due to the nature of the effective Hamiltonian.

We remark that the scope of this first analysis is the comparison between LR and cLR with respect to the corresponding SS approach and thus even low to medium level calculations such as CIS can be sufficient. By contrast, when the aim of the calculations is different (e.g., to compare computed excitation energies with experimental data), more advanced QM methods should be used as well as a larger attention should be paid to the presence of specific solute-solvent interactions, which are not correctly described by a continuum solvation model but require hybrid discrete/continuum methods.[28] Results are shown in Table I. $\Delta E_{\text{GS}}^{K0}$ is calculated as reported in Sec. II C, whereas SS values have been taken from the same reference.[13]

As already discussed in such a paper, the three excitations show a different behavior passing from a LR to a SS approach. The nature of this behavior can be correlated with the differences between the changes in the dipole moment passing from the ground state to the excited state ($\Delta\mu=|\mu_K-\mu_{\text{GS}}|$) and the transition dipole moment $\mu_{\text{GS},K}$. In the same paper, the conclusion of such analysis confirmed that if $2\mu_{\text{GS},K}^2$ is larger than $\Delta\mu^2$, the LR excitation energy is smaller than the SS one, and vice versa.

As shown in Table I, for all excitations, the cLR values represent a change of the LR result towards a better agreement with SS, and in one case (MCP in dioxane) the cLR model is able to recover the red solvatochromism found with the SS model which was lost in the LR scheme, where a blueshift was obtained. It is important to note that the increment in the computational effort of the cLR approach with respect to the standard LR calculation is almost negligible.

For the parallel analysis on TDDFT, we report a graphical representation (Fig. 1) as this can be directly compared with the graphs reported in the reference paper.[13]

Here we cannot refer to SS results as reference, but still we can estimate the accuracy of the cLR method with respect

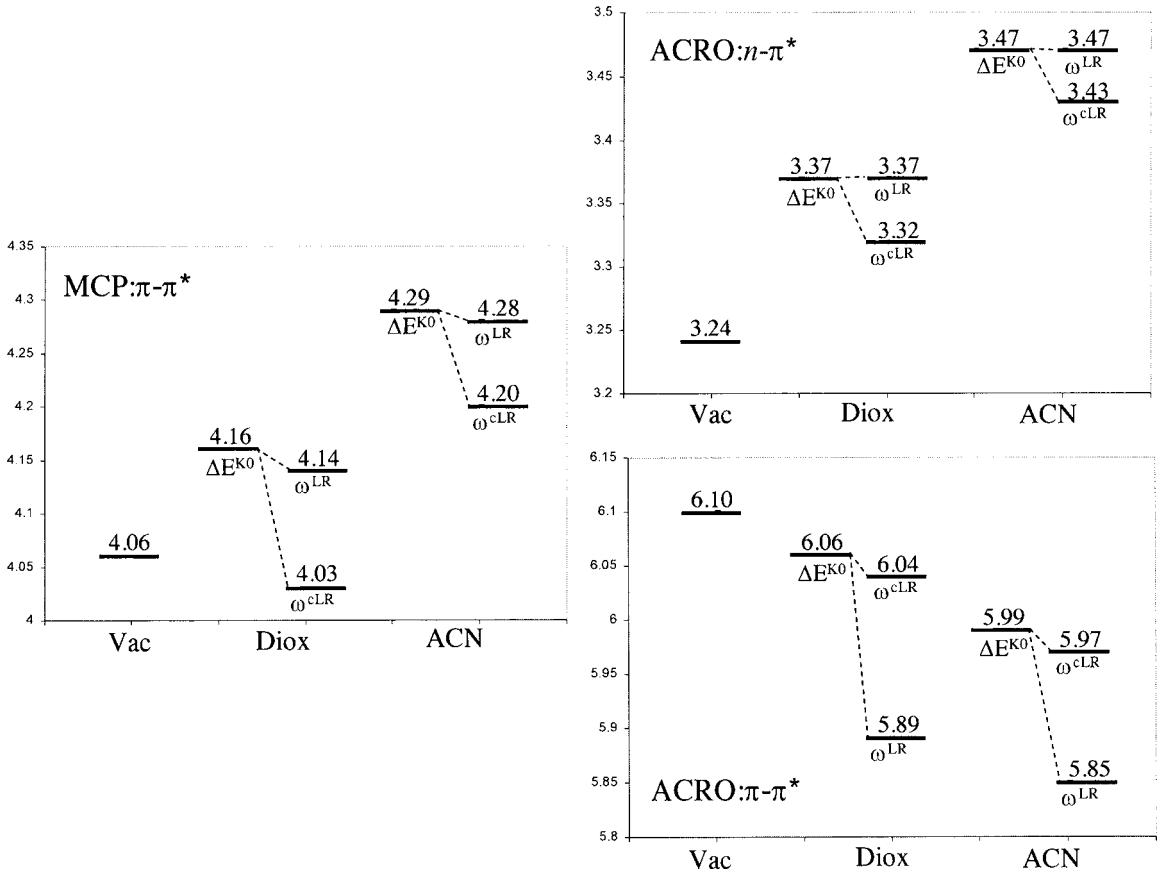

FIG. 1. Graphical representation of the TDDFT results obtained using either the linear response (LR) or the corrected linear response (cLR) approach for the absorption energies of MCP and ACRO in gas phase, in dioxane, and in acetonitrile. Values are in eV.

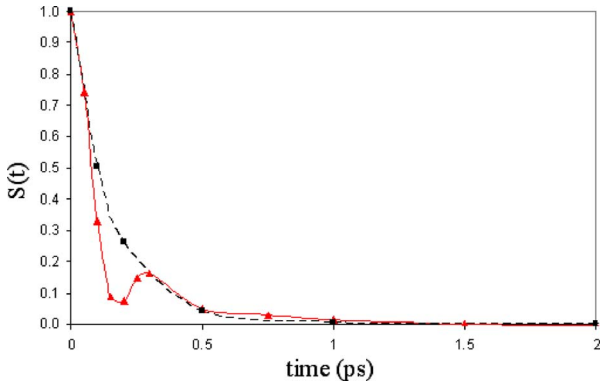

FIG. 2. TDSS functions for MCP calculated at the TDDFT level using the Debye (black) and the fit (red) models for $\hat{\varepsilon}(\omega)$.

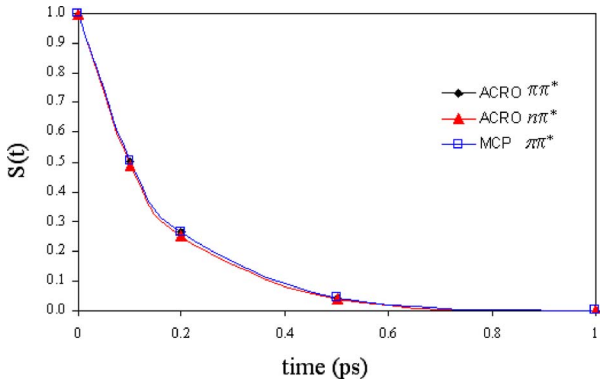

FIG. 3. TDSS functions for MCP and for the two transitions of ACRO calculated at the TDDFT level using the Debye model for $\hat{\varepsilon}(\omega)$.

to LR by comparing with the CIS results. Indeed, the behavior found passing from LR to cLR is equivalent to that obtained at the CIS level. The correction introduced in the cLR approach with respect to the standard LR leads to a decrease in the excitation energies of both the $\pi \rightarrow \pi^*$ transition of MCP (and in dioxane this implies a redshift with respect to a blueshift) and the $n \rightarrow \pi^*$ transition of ACRO and an increase in the second $\pi \rightarrow \pi^*$ transition of ACRO. Once again, this is the result one expects from the analysis of the differences between the changes in the dipole moment of each state and the transition dipole moments; in fact, for MCP $\pi \rightarrow \pi^*$ and for ACRO $n \rightarrow \pi^*$ the dipole moment difference $\Delta\mu$ is large, while the transition dipole moment $\mu_{\mathrm{GS},K}$ is small (or null); the opposite behavior is valid for the $\pi \rightarrow \pi^*$ transition in ACRO.

B. Time dependent Stokes shift

In this section we report the results obtained for TDSS quantities defined in Sec. III B. For this study, two alternative expressions of $\hat{\varepsilon}(\omega)$ have been tested, one taken from a combination of fitted experimental data in the high frequency region and of the Debye-type relaxation in the low frequency region (from now on indicated as fit), and one modeled on a purely diffusive Debye relaxation (from now on indicated as Debye). Differences between the two $\hat{\varepsilon}(\omega)$ are reported in Fig. 2, where the results obtained for the TDSS defined in Eq. (29) are displayed for MCP transition. By definition, the TDSS values vary from 1 to 0.

One feature of the fit curve obtained with a combined Debye+exp, not observed in the Debye-only model, is the initial Gaussian decay and the following oscillations.[29–31] At sufficiently short times, the motions of molecules can be considered as independent of intermolecular interactions; the frequency which characterizes the initial Gaussian decay of the solvation energy thus reflects the "free streaming" of solvent molecules uncoupled from one another. This free-streaming motion represents the first phase of solvation. The oscillations, on the other hand, represent collective dynamics occurring in an intermediate time regime. Within this phase of solvation molecules are colliding with their neighbors (and the solute) and rebounding in a relatively coherent fashion for some length of time, exhibiting a behavior similar to that of an underdamped oscillator. However, these oscillations die out relatively quickly and the diffusive contribution to the overall response becomes predominant. In this time scale, the two curves follow similar decay rates.

Figure 3 shows the TDSS for MCP and for the two transitions of ACRO in acetonitrile obtained using the Debye model in all cases. The perfect equivalence of three plots reported in the figure shows that the TDSS is a property of the solvent and thus is almost independent on the solute.

Although the plots in Figs. 2 and 3 can be used as an internal check for the reliability of the relaxation model presented in Sec. III B, they carry less information than the explicit consideration of the excited and ground state curves, as defined in Eqs. (27) and (30), respectively. This becomes evident when Figs. 4–6 are considered. They show the time evolution of the excited state free energy $\mathcal{G}_K(t)$ and the corresponding emission energies to the vertical ground state (represented as arrows) for MCP and for the two transitions in ACRO, respectively. All the energies are referred to the ground state equilibrium free energy of the corresponding molecule. The $\mathcal{G}_K(t)$ curves for MCP are computed using both the Debye and fit models for the frequency dependent permittivity $\hat{\varepsilon}(\omega)$, while those for the two ACRO transitions are obtained using the Debye model only.

For all the systems the excited state free energy curves $[\mathcal{G}_K(t)]$ are similar; in all systems in fact the initial time $t=0$ corresponds to a vertical excitation from the ground state to a nonequilibrium excited state that then relaxes towards a new equilibrium characterized by a lower energy. For MCP, when using the fit model we can observe the same pattern found for the TDSS function, in which at short times the decay is of Gaussian type, followed by oscillations, and finally, assuming the typical diffusive character. The equivalence of the excited state curves is also reflected in the corresponding vertical ground state curves. For these latter, the definition of the proper free energy function is given in Eq. (30).

Passing to describe the behavior of the emission energies, we observe different results for the three transitions. For MCP, the emission energies vary by 0.3 eV from $t=0$ to $t=\infty$, while for ACRO a much smaller variation is found, namely, 0.11 and 0.065 eV for the $n \rightarrow \pi^*$ and $\pi \rightarrow \pi^*$ transitions, respectively. This behavior can be explained considering the different character of the electronic states involved.

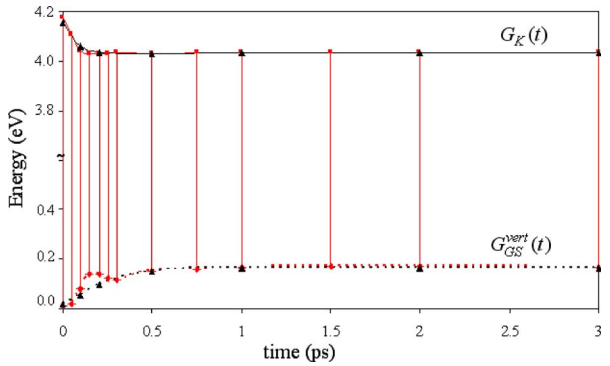

FIG. 4. Time dependent evolution of the excited state free energy $\mathcal{G}_K(t)$ (in eV) of MCP calculated at the TDDFT level using the Debye (dotted) and the fit models for $\hat{\varepsilon}(\omega)$. For the latter, we also report the transition energies towards the vertical ground state at the various times. All the energies are referred to the ground state equilibrium free energy.

In the excited state of MCP (Fig. 4) the dipole moment points in the opposite direction with respect to the ground state, while its intensity is not subject to significative variations. At short times, when the inertial charges $\mathbf{q}_K^{\text{in}}(t)$ determining the energy of the vertical ground state [see Eq. (30)] have had not time to relax but still resemble the initial ground state, the vertical state is close to the equilibrium value $\mathcal{G}_{\text{GS}}$. At longer times, the solvent charges $\mathbf{q}_K^{\text{in}}(t)$ have had time to change according to the excited state charge distribution of the solute, and the vertical ground state becomes more and more different from the equilibrium value $\mathcal{G}_{\text{GS}}$. This net variation of the solvent reaction field in the two states is thus reflected in the significant decrease of the emission energy with the solvent relaxation.

For the $n \rightarrow \pi^*$ transition of ACRO (Fig. 5), the excited state is less polar than the ground state, but the direction of the dipole moment remains the same. At short times, the influence of the more polar ground state, still dominant in the inertial part of the solvent charges, makes the energy of the vertical ground state close to $\mathcal{G}_{\text{GS}}$, while the difference between the two functions increases as the solvent charges relax towards the solute excited state charge distribution. However, in this case, the change in the solvent effect on the emission is significantly smaller than in MCP.

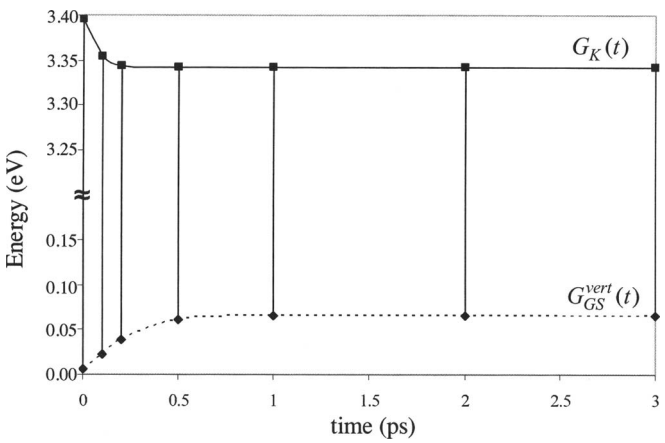

FIG. 5. Time dependent evolution of the $n \rightarrow \pi^*$ excited state free energy $\mathcal{G}_K(t)$ (in eV) of ACRO calculated at the TDDFT level using the Debye model for $\hat{\varepsilon}(\omega)$. The arrows indicate transition energies towards the vertical ground state at various times. All the energies are referred to the ground state equilibrium free energy.

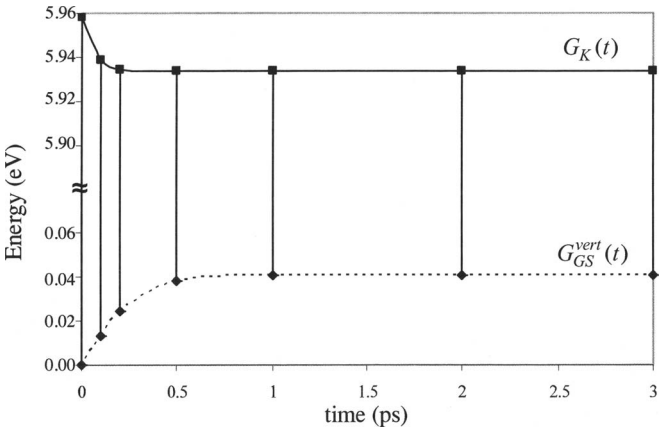

FIG. 6. Time dependent evolution of the $\pi \rightarrow \pi^*$ excited state free energy $\mathcal{G}_K(t)$ (in eV) of ACRO calculated at the TDDFT level using the Debye model for $\hat{\varepsilon}(\omega)$. The arrows indicate transition energies towards the vertical ground state at various times. All the energies are referred to the ground state equilibrium free energy of the corresponding molecule.

Finally, for the $\pi \rightarrow \pi^*$ transition of ACRO (Fig. 6), the two states have a similar charge distribution (with the excited state being slightly more polar than the ground state). As a consequence, the energy of both excited state and vertical ground state will not significantly change with the relaxation of the solvent.

Through all the examples reported in this section we showed that, by explicitly considering the PCM time dependent charges, one can obtain information about the effects of the solvent relaxation on the solute electronic states. By contrast, the standard analysis of the TDSS function will only give information on the solvent relaxation independently of the solute.

A further example of the potentialities of the TDPCM model will be given in the following section.

C. Cyclic relaxation

In this section we present the results for the cyclic relaxation process of MCP, as discussed in Sec. III C.

Figure 7 shows the six steps in which we have divided the process. For this analysis the solvent relaxation has been described using the Debye model for the frequency dependent permittivity. The range of t in which we have followed the solvent relaxation (3 ps for the excited state and 3 ps for the ground state) is arbitrary, and it represents a time interval which is large enough to ensure that the relaxation of the solvent is complete. In the figure the energy changes due to solute geometry relaxation are indicated as dotted arrows; this is just a graphical simplification as these changes happen in a different time scale with respect to that represented by the solvent relaxation and a three-dimensional (3D) plot should be used.

The comparison of Figs. 7 and 4 shows the differences between the ground states involved in the two processes. Here the ground state energy curve is completely determined by the solvent relaxation from the initial vertical nonequilibrium state (at $t=3$ ps) towards the final equilibrium ground

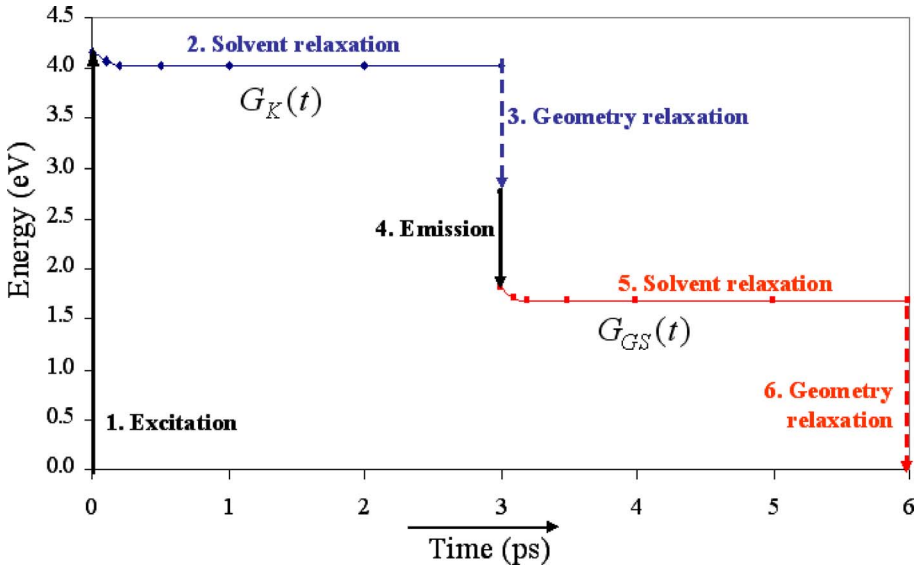

FIG. 7. Graphical representation of the six steps of the cyclic relaxation of MCP. The full arrows indicate the vertical transitions from the equilibrated ground state to the nonequilibrium excited state (*excitation*) and from the equilibrated excited state to the nonequilibrium ground state (*emission*). The dotted arrows indicate the energy changes due to the solute *geometry* relaxation.

state at $t=6$ ps, while in Fig. 4 the ground state reached at each time t was represented by the vertical (or nonequilibrium) $\mathcal{G}_{GS}^{vert}(t)$ of Eq. (30). We note that also at $t=3$ ps, i.e., the only point at which the ground states in the two figures should be equivalent (they both represent a vertical state from an equilibrated excited state), the $\mathcal{G}_{GS}$ value in Fig. 7 is different (higher) from the corresponding $\mathcal{G}_{GS}^{vert}$ value in Fig. 4; the two energies are in fact calculated at different geometries, the geometry of the excited state and of the ground state, respectively.

The analysis of the curves in Fig. 7 also shows the relative importance of the solute geometry relaxation and the solvent dielectric relaxation. In fact, even for a quite rigid system as the MCP, the dielectric relaxation accounts for few tenths of eV, while the relaxation of the solute geometry accounts for more than 1 eV for the excited state and more than 1.5 eV for the ground state.

To better appreciate these geometry effects, we give here some more details on such calculations. The geometry optimization for the excited state has been performed using the TDDFT energy gradients recently implemented in the development version of the GAUSSIAN package.[19]

As already noted the dipole moments of the ground state and of the excited state lie along the C_3-C_4 bond (see Fig. 8 for the numeration of atoms), have similar magnitude (when computed at the geometry of the ground state they are 2.498 and 3.090 D, respectively), but they point towards opposite directions. This characteristic behavior of MCP is also reflected in the main geometry changes passing from the ground to the excited state. The C_1-C_2 and C_3-C_4 double bonds become larger in the excited state ($\Delta_{12}=+0.21$ Å and $\Delta_{34}=+0.10$ Å, respectively), while the C_2-C_3 bond becomes shorter ($\Delta_{23}=-0.08$ Å), indicating that in the excited state there is a partial charge transfer towards the ring. Moreover, the hydrogens bonded to C_1 and C_2 go out of the molecular plane.

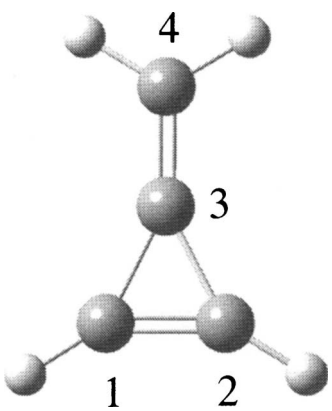

FIG. 8. Structure of MCP with an indication of the numeration used to distinguish the carbon atoms.

As noted at the end of the previous section, the TDPCM not only allows the evaluation of the changes in the energies of the electronic states, but it can also be used to study the evolution of the solute properties. As a simple but indicative example, in Fig. 9 we report the time dependent evolution of the Mulliken charges on the carbon atoms for both the excited state and the ground state (the charges are calculated with respect to the corresponding initial states, namely, the vertical excited state a $t=0$ and the vertical ground state after excited state geometry relaxation).

The graphs reported in figure clearly show the contribution of the solvent to the redistribution of the charge density in the two electronic states following vertical absorption and emission, respectively. As observed for the geometry changes, the excited state is characterized by a flux of electronic charge from the C_3-C_4 bond towards the ring; the effect of the solvent relaxation is to amplify such a flux, as shown by the positive values of the change in the C_4 and C_3 charges which increase with time, and the parallel increase of negative charge on the C_2 and C_1 atoms. For the ground state, a reversed phenomenon is observed, with a net time dependent increase of the electronic charge in the C_4 atom.

V. CONCLUDING REMARKS

In this paper a novel approach to study the formation and relaxation of excited states in solution is presented within the IEF version of the polarizable continuum model. Such an

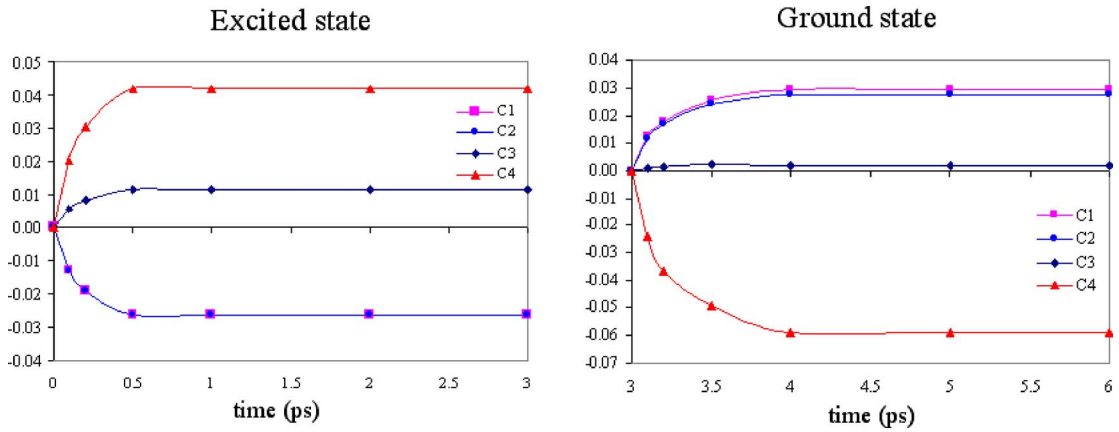

FIG. 9. Graphical representation of the time dependent evolution of the Mulliken atomic charges (in a.u.) on the carbons of MCP for the excited (left) and the ground (right) states. All the values are referred to the nonequilibrium values, i.e., the values calculated in the vertical excited and ground states, respectively.

approach uses the excited state relaxed density matrix to correct the TDDFT excitation energies and it introduces a state-specific (SS) solvent response which can be further generalized within a time dependent formalism. This generalization is based on the use of a complex dielectric permittivity as a function of the frequency, $\hat{\varepsilon}(\omega)$.

The approach is here presented in its theoretical formulation and applied to the various steps involved in the formation and relaxation of electronic excited states in solvated molecules, starting from the vertical excitation from an equilibrated solute-solvent system and considering the following relaxation in both the solute geometry and the solvent polarization. In particular, two applications have been presented: (1) the time dependent Stokes shift (TDSS), as a quantity experimentally measurable and which gives information on the decay of the inertial polarization of the solvent; and (2) the cyclic process beginning with a vertical excitation from an equilibrated solute-solvent system and terminating back to the same system, passing through solvent and solute relaxation.

These two applications have been selected to show the potentialities of the method. In fact, the first one involves the solvent internal modes activated by a perturbation, as a consequence of electrostatic solute-solvent interactions. In our model, the definition of TDSS only depends on the way we describe the solvent response and it is therefore a property of the solvent, in the approximation that the solute geometry relaxation is much slower than the solvent one. In fact, by performing calculations on different probe solutes in the same solvent, the same TDSS function has to be obtained. On the other hand, the cyclic process (starting from an equilibrated GS, passing through an excited state, and then going back to the initial equilibrium) involves both the solute and the solvent, and it strongly depends on their interactions. In this case, an important role can be played by solute geometry relaxation effects. In our model, these effects have been completely decoupled from those of the solvent relaxation, however, an estimation of the relative magnitude of the two contributions to the overall time dependent interaction has been given.

As can be seen, the corrected LR model and its extension to time dependent solvation open a wide range of possible studies going from spectroscopies to photochemistry. This large set of applications however also leads to many specific aspects to be accounted for and thus to the necessity to extend the basic model we have presented here along different directions: some of these extensions are at present under elaboration,[3,18] but many others will require longer periods to reach maturity.

ACKNOWLEDGMENT

Financial support by Gaussian Inc. is here acknowledged by five of the authors (M.C., B.M., J.T., R.C., and G.S.).

[1] J. Tomasi and M. Persico, Chem. Rev. (Washington, D.C.) **94**, 2027 (1994).
[2] C. J. Cramer and D. G. Truhlar, Chem. Rev. (Washington, D.C.) **99**, 2161 (1999).
[3] J. Tomasi, B. Mennucci, and R. Cammi, Chem. Rev. (Washington, D.C.) **105**, 2999 (2005).
[4] B. Mennucci, R. Cammi, and J. Tomasi, J. Chem. Phys. **109**, 2798 (1998).
[5] R. Cammi and B. Mennucci, J. Chem. Phys. **110**, 9877 (1999); R. Cammi, B. Mennucci, and J. Tomasi, J. Phys. Chem. A **104**, 5631 (2000).
[6] M. Cossi and V. Barone, J. Chem. Phys. **115**, 4708 (2001).
[7] M. V. Basilevskyi, D. F. Parsons, and M. V. Vener, J. Chem. Phys. **108**, 1103 (1998).
[8] I. V. Rostov, M. V. Basilevsky, and M. D. Newton, in *Simulation and Theory of Electrostatic Interactions in Solution*, edited by L. R. Pratt and G. Hummer (American Institute of Physics, New York, 1999).
[9] P. G. Wolynes, J. Chem. Phys. **86**, 5133 (1987).
[10] M. D. Newton and H. L. Friedman, J. Chem. Phys. **88**, 4460 (1988).
[11] C. P. Hsu, X. Song, and R. A. Marcus, J. Phys. Chem. B **101**, 2546 (1997).
[12] F. Ingrosso, B. Mennucci, and J. Tomasi, J. Mol. Liq. **108**, 21 (2003).
[13] R. Cammi, S. Corni, B. Mennucci, and J. Tomasi, J. Chem. Phys. **122**, 104513 (2005).
[14] S. Corni, R. Cammi, B. Mennucci, and J. Tomasi, J. Chem. Phys. **123**, 134512 (2005).
[15] E. Cancès, B. Mennucci, and J. Tomasi, J. Chem. Phys. **107**, 3032 (1997); B. Mennucci, E. Cancès, and J. Tomasi, J. Phys. Chem. B **101**, 10506 (1997).
[16] S. Miertus, E. Scrocco, and J. Tomasi, Chem. Phys. **55**, 117 (1981); R. Cammi and J. Tomasi, J. Comput. Chem. **16**, 1449 (1995).
[17] M. Caricato, F. Ingrosso, B. Mennucci, and J. Tomasi, J. Chem. Phys. **122**, 154501 (2005).
[18] B. Mennucci, Theor. Chem. Acc. (in press).
[19] G. Scalmani, M. Frisch, B. Mennucci, J. Tomasi, R. Cammi, and V. Barone, J. Chem. Phys. **124**, 094107 (2006).
[20] G. Scalmani, V. Barone, K. N. Kudin, C. S. Pomelli, G. E. Scuseria, and

M. J. Frisch, Theor. Chem. Acc. **111**, 90 (2004).
[21] This approximation is introduced here as it allows a more compact notation; we note, however, that in the computational code both formulations have been implemented and that numerical tests have shown an almost exact equivalence. We also remark that in the limit of an exact solution of the electrostatic problem, Eq. (8) is exactly fulfilled.
[22] F. Furche and R. Ahlrichs, J. Chem. Phys. **117**, 7433 (2004).
[23] C. Van Caillie and R. D. Amos, Chem. Phys. Lett. **308**, 249 (1999); **317**, 159 (2000).
[24] N. C. Handy and H. F. Schaefer III, J. Chem. Phys. **81**, 5031 (1984).
[25] M. J. Frisch, G. W. Trucks, H. B. Schlegel *et al.*, GAUSSIAN Development Version, Revision D.02, Gaussian, Inc., Wallingford, CT, 2004.
[26] C. J. F. Böttcher and P. Bordewijk, *Theory of Electric Polarization* (Elsevier, Amsterdam, 1978), Vol. 2.
[27] G. R. Fleming and M. Cho, Annu. Rev. Phys. Chem. **47**, 109 (1996).
[28] For acroleina see, for example, F. Aquilante, V. Barone, and B. O. Roos, J. Phys. Chem. A **119**, 12323 (2003); S. Andrade do Monte, T. Muller, M. Dallas, H. Lischka, M. Diedenhofen, and A. Klamt, Theor. Chem. Acc. **111**, 78 (2004); whereas for MCP R. Cammi, L. Frediani, B. Mennucci, J. Tomasi, K. Ruud, and K. V. Mikkelsen, J. Chem. Phys. **117**, 13 (2002); K. B. Wiberg and Y.-G. Wang, J. Phys. Chem. A **108**, 9417 (2004).
[29] R. Jimenez, G. R. Fleming, P. V. Kumar, and M. Maroncelli, Nature (London) **369**, 471 (1994).
[30] M. L. Horng, J. A. Gardecki, A. Papazyan, and M. Maroncelli, J. Phys. Chem. **99**, 17311 (1995).
[31] B. M. Ladanyi and S. D. Schwartz, *Theoretical Methods in Condensed Phase Chemistry* (Kluwer, Dordrecht, The Netherlands, 2000).